# JARID2 and the PRC2 complex regulate the cell cycle in skeletal muscle

Abhinav Adhikari, Pramish Mainali, and Judith K. Davie[1]

*From the Department of Biochemistry and Molecular Biology and Simmons Cancer Institute, Southern Illinois University School of Medicine, Carbondale, Illinois 62901*

Edited by Joel M. Gottesfeld

JARID2 is a noncatalytic member of the polycomb repressive complex 2 (PRC2) which methylates of histone 3 lysine 27 (H3K27). In this work, we show that JARID2 and the PRC2 complex regulate the cell cycle in skeletal muscle cells to control proliferation and mitotic exit. We found that the stable depletion of JARID2 leads to increased proliferation and cell accumulation in S phase. The regulation of the cell cycle by JARID2 is mediated by direct repression of both cyclin D1 and cyclin E1, both of which are targets of PRC2-mediated H3K27 methylation. Intriguingly, we also find that the retinoblastoma protein (RB1) is a direct target of JARID2 and the PRC2 complex. The depletion of JARID2 is not sufficient to activate RB1. However, the ectopic expression of RB1 can suppress cyclin D1 expression in JARID2-depleted cells. Transient depletion of JARID2 in skeletal muscle cells leads to a transient up-regulation of cyclin D1 that is quickly suppressed with no resulting effect on proliferation, Taken together, we show that JARID2 and the PRC2 complex regulate skeletal muscle proliferation in a precise manner that involves the repression of cyclin D1, thus restraining proliferation and repressing RB1, which is required for mitotic exit and terminal differentiation.

Cell proliferation and differentiation are mutually exclusive but closely coordinated and highly regulated processes. In skeletal muscle, the process is marked by a large number of gene expression changes as cell cycle genes go from highly expressed to permanently silenced while another set of genes that are normally repressed during proliferation are activated during differentiation (1).

Two essential protein families that regulate the cell cycle are cyclins and cyclin-dependent kinases (CDKs).[2] These complexes guide the transition of cells through the different phases of the cell cycle. In the mammalian system, cyclins D and E govern the progress through the $G_1$/S phases whereas the mitotic cyclins A and B promote progression through the $S/G_2/M$ phases of the cell cycle (2). Mitogenic signaling stimulates the synthesis and assembly of the short-lived D-type cyclins with CDK4 or CDK6 (3). Cyclin D/CDK complexes are active as long as mitogenic stimulation continues. Cyclin D/CDK acts directly as a kinase to phosphorylate cellular substrates critical for cell cycle progression. D-type cyclins also act to sequester the CDK inhibitors p27 and p21 in a kinase-independent role (2). The protein level of cyclin E is maximum at the $G_1$/S transition and is followed by an increase in cyclin A levels during S phase. Both cyclin A and E can form complexes with CDK2, although CDK1 can only form a complex with cyclin A. Rising levels of cyclin B result in the induction of CDK1 at the $G_2$/M phase. Coordinated cell cycle progression is a result of the highly regulated fluctuation in the expression of cyclins and activation of cognate CDKs (reviewed in Ref. 1).

Skeletal muscle determination and differentiation are controlled by four highly related basic-helix-loop-helix transcription factors known as the myogenic regulatory factors (MRFs) which include Myf5 (*Myf5*), MyoD (*Myod*), myogenin (*Myog*), and MRF4 (*Myf6*) (4–6). MyoD and Myf5 have been shown to promote the proliferation of muscle progenitor cells whereas myogenin appears to possess the intrinsic activity required to mediate cell cycle exit as the exogenous expression of myogenin in proliferating myoblast causes premature exit of myoblast from the cell cycle (7). MyoD can also promote cell cycle arrest by induction of the cyclin-dependent kinase inhibitor p21 (8, 9) along with other Cip1/Kip1 family members, p57 and p27, which inhibit a wide range of CDKs essential for cell cycle progression (10). During differentiation, the induction of p21 is followed by the expression of myogenin, which marks a "point of no return" for mitotic exit. High levels of p21 are required for maintenance of the post–mitotic state in differentiated myoblasts and MyoD can also induce RB1 expression (11).

In skeletal muscle, the retinoblastoma protein (pRB, RB1) has a critical role in negative regulation of cell cycle progression by promoting exit from the cell cycle and maintaining the differentiated state (12–14). RB1 maintains cell cycle arrest, which is required for skeletal muscle differentiation, in part by regulating the activity of the E2F family of transcription factors. Pocket proteins, a family that includes RB1 as well as related p107 and p130 proteins, bind and repress E2F activity (12). Activation of cyclin D and CDK4/6 proteins by mitogen-rich conditions allows monophosphorylation of pocket proteins which releases bound activator E2F transcription factors from

hypophosphorylated RB1 proteins. Thus, cyclin D/CDK expression results in activation of E2F target cell cycle genes including cyclin E. Cyclin E, in complex with CDK2, further hyperphosphorylates RB1 proteins into the hyperphosphorylated inactive form of RB1 which allows cells to progress through the $G_1$/S restriction point (reviewed in Refs. 15 and 16).

Polycomb repressor proteins have an important developmental role and play essential roles in skeletal muscle. The two major polycomb complexes, Polycomb Repressive Complex-1 (PRC1) and Polycomb Repressive Complex-2 (PRC2), are responsible for the ubiquitination of lysine 119 of histone H2A (H2AK119) (17) and the methylation of lysine 27 on histone H3 tail (H3K27), respectively (18–20). The methylation of H3K27 by PRC2 requires one of the SET domain–containing enhancer of zeste proteins, EZH1 or EZH2. Promoters and enhancers of many lineage-specific genes contain dimethylated and trimethylated H3K27, and the methylation profile of many of these genes is lost upon differentiation (reviewed in Ref. 21).

JARID2, a founding member of Jumonji family of histone demethylases, has no detectable histone demethylase activity and yet is evolutionarily conserved from *Drosophila* to human (Ref. 22, reviewed in Ref. 23). Recently, it has been shown to be a substoichiometric component of PRC2 which aids in targeting PRC2 and is required for embryonic stem cell differentiation (24). In mice, JARID2 was found to be essential for heart development (25). JARID2 mutant mice exhibit various neural tube, cardiac, and hematopoietic defects and die *in utero* because of cardiac and hematopoietic defects (26). In cardiac cells, JARID2 has been shown to control the cell cycle through regulation of cyclin D1 (25, 27, 28). However, the role of JARID2 in skeletal muscle development and regeneration is not well-understood.

We have recently shown that loss of JARID2 blocks differentiation in C2C12 cells through the modulation of the canonical Wnt signaling pathway (29). Here, we examined the effect of JARID2 on the proliferation of skeletal muscle cells. We found that depletion of JARID2 increased the proliferation rate and caused de-repression of positive cell cycle regulators like cyclin D1 and cyclin E1, whereas the negative cell cycle regulators like p21 and RB1 were down-regulated. JARID2 has been shown to recruit the histone methyltransferases G9a and GLP to directly regulate cyclin D1 in cardiomyocytes (30). We show here that JARID2 recruits the PRC2 complex to repress cyclin D1 and cyclin E1 in skeletal muscle and results in H3K27 methylation of target promoters. In a related study, we also have found that the modest depletion or chemical inhibition of EZH2 promotes proliferation through the JARID2-directed regulation of cyclin D1 and cyclin E1.[3] We also show that *Rb1* is a direct target of JARID2 and the PRC2 complex, but loss of repression by PRC2 is not sufficient to de-repress gene expression. The differentiation block with consequential increase in proliferation could be restored by exogenous expression of JARID2. Together, we show that JARID2 regulates the cell cycle in PRC2-dependent manner in skeletal muscle cells.

---

[3] A. Adhikari and J. K. Davie, submitted for publication.

## Results

### JARID2-depleted cells have increased proliferation

To understand the function of JARID2 in skeletal muscle proliferation, we established cell lines depleted for JARID2 with three independent shRNA constructs in C2C12 cells (29), a well-established *in vitro* differentiation model. mRNA and protein confirmation of one JARID2 depletion line derived from each shRNA construct is shown in Fig. S1. All described experiments were performed in two cell lines depleted with independent shRNA constructs (shJarid2-1 and shJarid2-3), and the results were consistent. For clarity, only the results for one shRNA construct (shJarid2-3) are shown. We assayed for the proliferation rate of these cells, and we found that C2C12 cells depleted for JARID2 proliferated significantly faster than cells with the scrambled control (Fig. 1A). To determine whether increased DNA synthesis was correlated with the enhanced proliferation observed, we performed an EdU incorporation assay for DNA synthesis and found that the number of actively proliferating cells marked by EdU incorporation was significantly higher in JARID2-depleted cells (Fig. 1B). To correlate the enhanced proliferation with changes in the cell cycle, the cell cycle state was assessed by flow cytometry following propidium iodide staining of the cells. We found that JARID2-depleted cells were much more highly enriched in the S phase at the expense of cells in the $G_1$ phase than the cells with a scrambled control, indicating that JARID2 plays a role in regulating the $G_1$/S transition (Fig. 1C and Fig. S2).

### JARID2 represses the positive cell cycle genes cyclin D1 and cyclin E1 to regulate the $G_1$/S transition

To understand how JARID2 was regulating the $G_1$/S transition, we examined the expression of factors that mediate this transition, including the gene encoding cyclin D1 (*Ccnd1*). *Ccnd1* is methylated at histone H3 lysine 27 in C2C12 cells in a PRC2-dependent manner upon differentiation (13). We found that *Ccnd1* mRNA was up-regulated in cells depleted for JARID2 (Fig. 2A), and this result was confirmed at the protein level as well (Fig. 2B). We next examined cyclin E1 (*Ccne1*), which functions in concert with cyclin D1 for the cells transition from $G_1$ to S phase. We found that cyclin E1, like cyclin D1, was also up-regulated at the level of mRNA (Fig. 2C) and protein (Fig. 2D). CDK4/6 and CDK2 are the CDKs that partner with cyclin D1 and cyclin E1, respectively, to phosphorylate various cellular substrates including the retinoblastoma protein (RB1) to regulate cell cycle progression. Thus, we also examined the expression of CDK2 and CDK4 and found that they were up-regulated at the mRNA level (Fig. 2, *E and G*) as well as the protein level (Fig. 2F).

### Stable loss of JARID2 results in repression of negative cell cycle regulators

The cyclin-dependent kinase inhibitor p21 and retinoblastoma proteins (RB1) are known negative regulators of cell cycle progression ($G_1$/S transition) and are key regulators of cell cycle exit. Thus, we assayed for the expression of RB1 (*Rb1*) and found that *Rb1* was severely down-regulated at the level of both mRNA (Fig. 3A) and protein (Fig. 3B). We also examined the
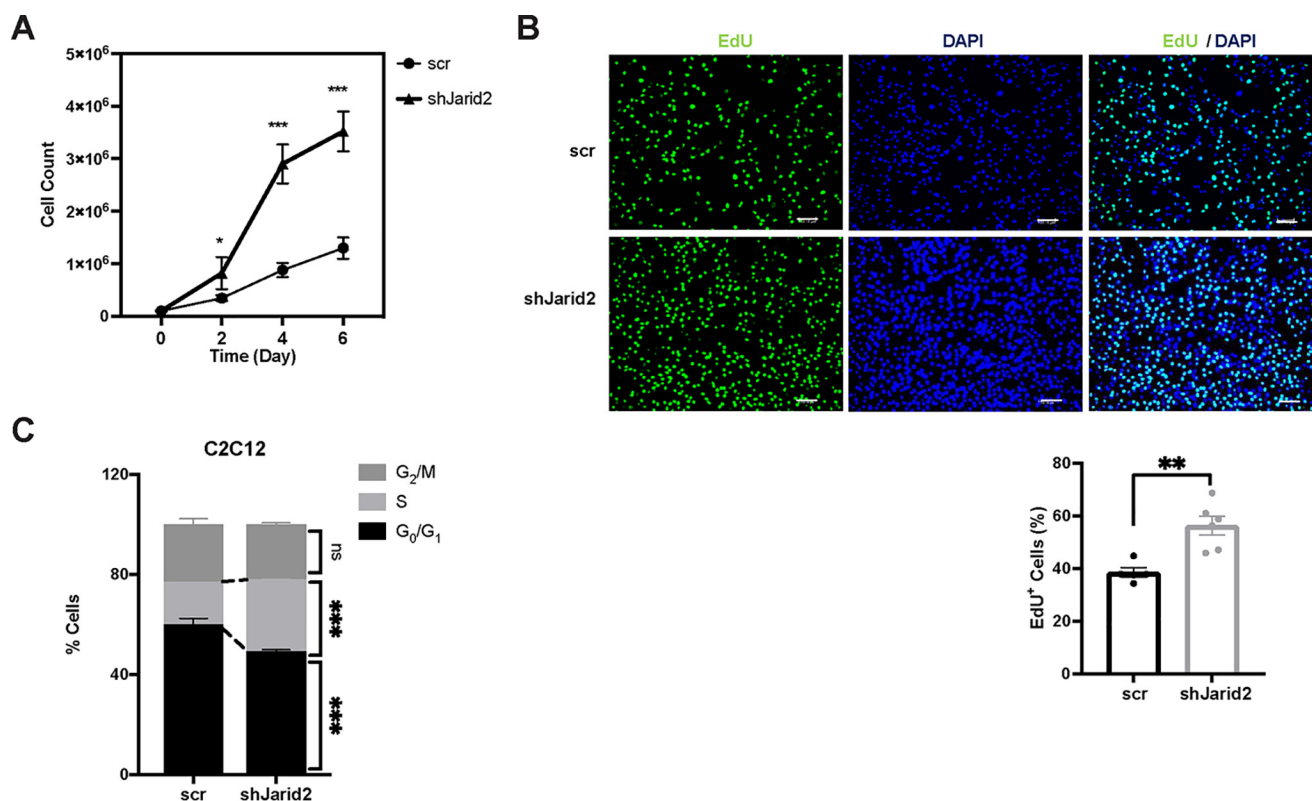
**Figure 1. JARID2 depletion results in increased proliferation and DNA synthesis in C2C12 cells.** *A*, an equal number of scrambled (scr) control or short-hairpin RNA against Jarid2 (shJarid2) expressing C2C12 cells were assayed for proliferation on the indicated days. *B*, scr and shJarid2 C2C12 cells were immunostained for EdU (*top panel*). Percent of EdU$^+$ nuclei were counted in at least five random fields and plotted (*bottom panel*). DAPI was used to stain nuclei. *Scale bar*, 100 $\mu$m; *n* = 3 biological replicates. *C*, loss of JARID2 increases the G$_1$/S transition during the cell cycle. Cells in *A* were ethanol fixed, propidium iodide stained, and analyzed for cell cycle phase distribution using flow cytometry. *Error bars*, mean ± S.E. (Student's *t* test; *ns* represents not significant; *, $p < 0.05$; **, $p < 0.01$; and ***, $p < 0.001$; *n* = 4 biological replicates.)

expression of p21 (*Cdkn1a*), which is also required for cell cycle exit. We found that *Cdkn1a* expression was inhibited at the mRNA level upon JARID2 depletion (Fig. 3C). The protein level was less severely affected, but the results show that *Cdkn1a* is not up-regulated upon the depletion of JARID2 (Fig. 3D).

### Exogenous expression of JARID2 restores cell proliferation defect in JARID2-depleted C2C12 cells

To confirm the dependence on JARID2, we asked if restoration of JARID2 could rescue the observed effects on the cell cycle regulators. Scr control and JARID2-depleted cells were transfected with an expression construct for JARID2 (pEF-Jarid2) or vector control (pEF). The expression of JARID2 was confirmed by mRNA (Fig. 4A) and protein (Fig. 4B) analysis. We found that restoration of JARID2 rescued the increased proliferation defect observed on the JARID2 depletion (Fig. 4C). We also found that restoration of JARID2 down-regulated cyclin D1 at the mRNA (Fig. 4D), and protein (Fig. 4E) level, thus confirming that JARID2 controls the expression of cyclin D1 in skeletal muscle cells. Restoration of JARID2 also suppressed the expression of *Ccne1* (Fig. 4F). *Cdk4* and *Cdk2* mRNA expression were restored by JARID2 expression as well (Fig. 4, *G* and *H*). This effect could also be observed at the protein level (Fig. 4I). Interestingly, expression of the negative cell cycle regulators, RB1 and p21, were also rescued, resulting in an up-regulation of expression (Fig. 4J).

### JARID2 directly represses cyclin D1 in PRC2-dependent manner

In cardiac cells, JARID2 represses *Ccnd1* though alterations in histone H3 lysine 9 (H3K9) methylation (30). To determine whether JARID2 directly repressed *Ccnd1* in skeletal muscle, chromatin immunoprecipitation (ChIP) assays were used to probe JARID2 recruitment to the *Ccnd1* promoter. We found that JARID2 was present on the *Ccnd1* promoter and that depletion of JARID2 reduced this association (Fig. 5A). We next examined the methylation of H3K9 (H3K9me) in cells with or without JARID2 and found no change in the H3K9me profile (Fig. 5B). The antibody used in these experiments was panmethyl H3K9 that recognizes all three states of H3K9 methylation. We next examined the methylation of H3K27 as JARID2 has been shown to direct the PRC2 complex to target genes (31, 32) and found that depletion of JARID2 led to a significant depletion of this modification (Fig. 5C). To confirm that this reduction was not because of a loss of total histone 3 (H3) at this promoter, we also examined H3 levels in this region and found that H3 levels were unaltered (Fig. 5C). We also assayed for the presence of the catalytic subunit of the PRC2 complex, EZH2, and we found that EZH2 was associated with the *Ccnd1* promoter and that the association was reduced when JARID2 was depleted (Fig. 5D). EZH2 has previously been shown to bind to the *Ccnd1* promoter in myotubes (13), but we show here that this can also be detected in myoblasts and importantly, the recruitment of EZH2 depends on JARID2. As a positive control
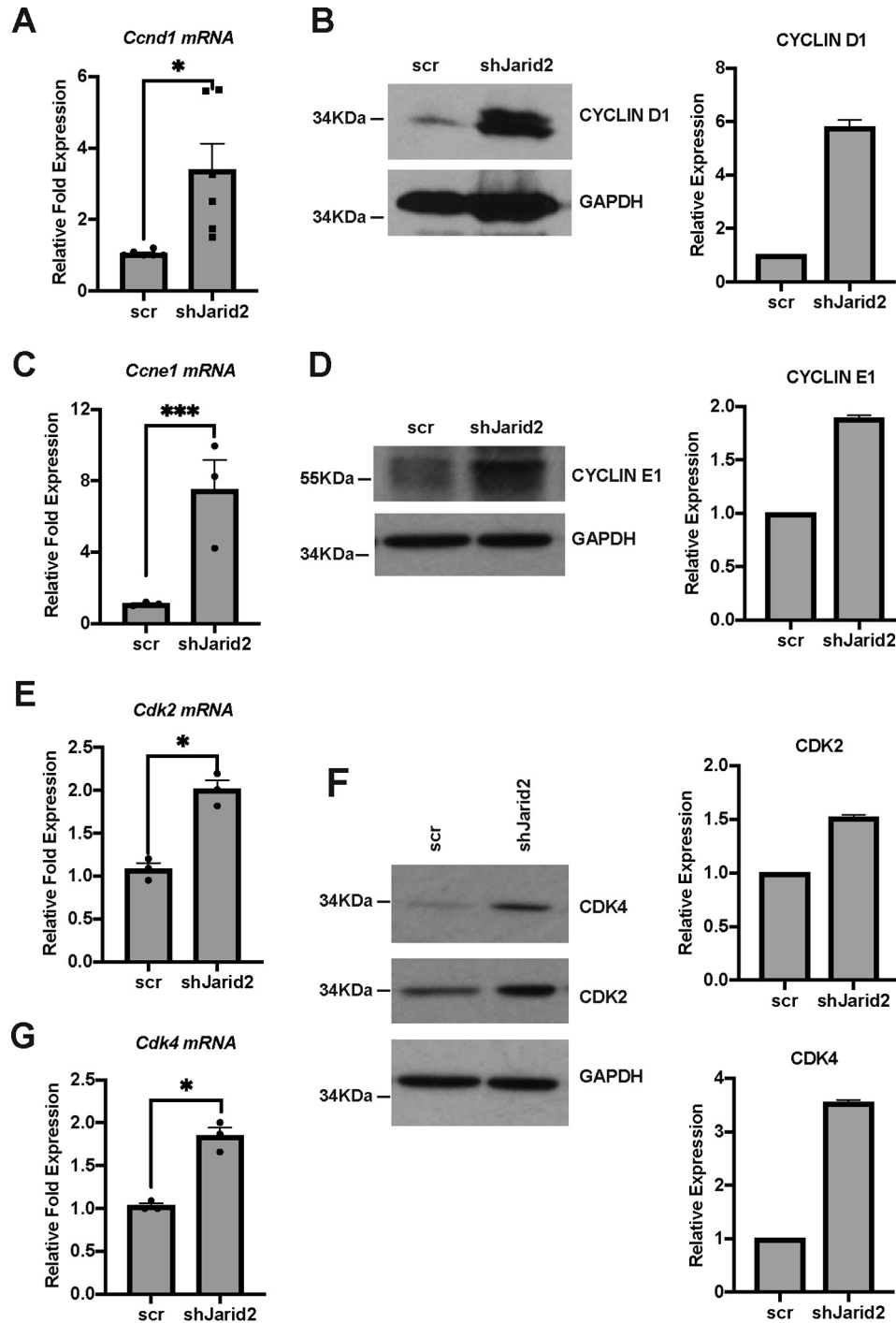
**Figure 2. JARID2 inhibits pro-proliferative cell cycle regulators.** *A* and *B*, JARID2 represses cyclin D1. Scrambled (scr) and shRNA expressing (shJarid2) C2C12 cells were assayed for cyclin D1 by qRT-PCR (*A*) and Western blotting (*B, left panel*). *B, right panel*, blots were quantified and plotted. Plots were normalized to GAPDH loading control. *C* and *D*, JARID2 also represses cyclin E1. As in *A*, cells were assayed for cyclin E1 by qRT-PCR (*C*) and Western blotting (*D, left panel*). *D, right panel*, blots in *C* were quantified and plotted. Plots were normalized to GAPDH loading control. *E–G*, JARID2 also represses cyclin-dependent kinases. Cells in *A* were assayed for Cdk2 and Cdk4 by qRT-PCR (*E* and *G*) and Western blotting (*F, left panel*). *D* and *F* were performed simultaneously and the same GAPDH blot was used. Blots in *F* were quantified and plotted. Plots were normalized to GAPDH (*F, right panel*). *Error bars*, mean ± S.E. (Student *t* test; *, $p < 0.05$ and ***, $p < 0.001$; $n = 3$–6 (qRT-PCR) and 3 (Western blots) biological replicates.)

for these experiments, we also examined the H3K27me3 status of the *Hoxb7* promoter, a well-established target of the PRC2 complex (33). H3K27me3 was highly enriched on the *Hoxb7* promoter and the depletion of JARID2 did not significantly disrupt this modification (Fig. 5E). Total H3 levels were also unaltered (Fig. 5E). The percentage input calculation shows that the

*Hoxb7* promoter is more highly enriched for H3K27me3 than *Ccnd1*, which may explain how the methylation of the *Ccnd1* and *Ccne1* promoters could have been overlooked in previous genome-wide studies. As a negative control, we also examined a promoter proximal region of *Tnni2* which we have previously shown is not a target of the PRC2 complex in proliferating cells
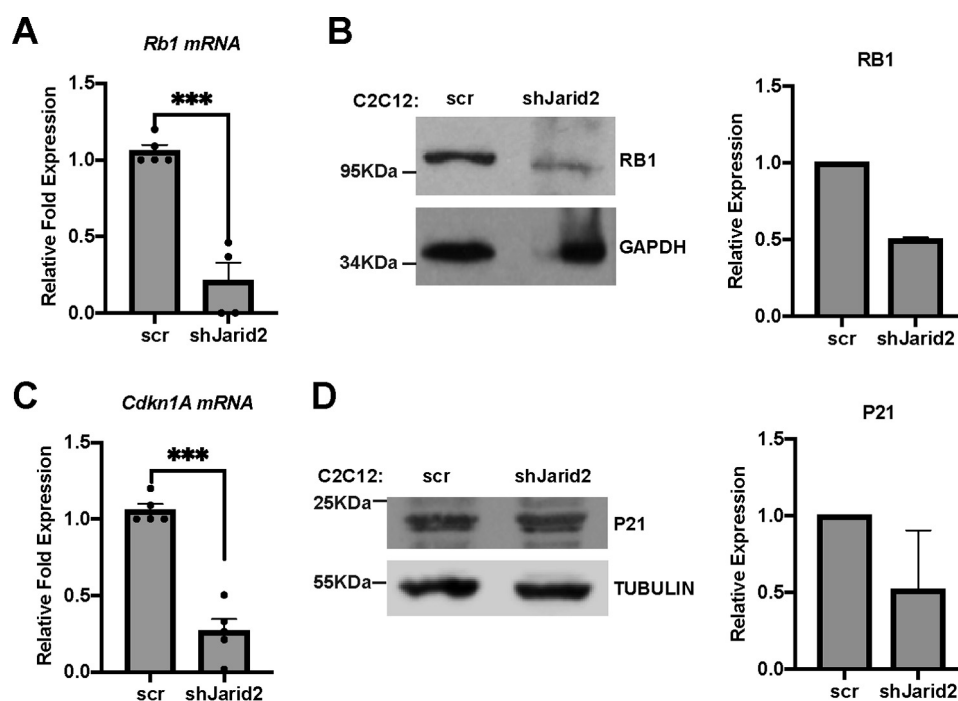
**Figure 3. Stable loss of JARID2 down-regulates negative cell cycle regulators in C2C12 cells.** *A* and *B*, RB1 is inhibited in JARID2-depleted cells. Proliferating scrambled (scr) and JARID2-depleted (shJarid2) C2C12 cells were assayed by qRT-PCR (*A*) and Western blotting assays (*B, left panel*). *B, right panel*, blots were quantified and plotted. Plots were normalized to GAPDH loading control. *C* and *D*, *Cdkn1a* (p21) is repressed in JARID2-depleted cells. Cells in *A* were assayed for p21 by qRT-PCR (*C*) and Western blotting (*D, left panel*). *C, right panel*, blots in *C* were quantified and plotted. Plots were normalized to TUBULIN loading control. *Error bars*, mean ± S.E. (Student's *t* test; ***, $p < 0.001$; $n = 5$ (qRT-PCR) and 3 (Western blots) biological replicates.)

(32). We found that JARID2 and EZH2 were not recruited to this region and H3K27me3 and H3K9me were not altered upon JARID2 depletion (Fig. 5*F*).

Cyclin D1 is an essential cell cycle regulator and is activated by several factors, including β-catenin, the effector of the canonical Wnt pathway. We have recently found that JARID2 directly represses an antagonist of the canonical Wnt signaling pathway, *Sfrp1*, which leads to an inhibition of the nuclear translocation of β-catenin in JARID2-depleted cells (29). To determine whether an alteration in β-catenin recruitment contributed to the activation of cyclin D1, we performed ChIP assays for β-catenin on the *Ccnd1* promoter. We found that β-catenin levels were reduced on the *Ccnd1* promoter upon JARID2 depletion (Fig. 5*G*). This result is consistent with our study showing the JARID2-dependent reduction in the nuclear translocation of β-catenin (29). This result also shows that the up-regulation of cyclin D1 observed is because of the loss of the JARID2/PRC2-dependent H3K27 methylation and not an enhanced recruitment of the activator β-catenin.

We next asked if *Ccne1* was also a direct target of JARID2 and the PRC2 complex. JARID2 was found to be associated with the *Ccne1* promoter, and JARID2 depletion reduced this association (Fig. 5*H*). Like *Ccnd1*, we found that H3K9 methylation on *the Ccne1* promoter was unchanged upon JARID2 depletion (Fig. 5*I*). We found that H3K27 methylation at the *Ccne1* promoter was reduced upon JARID2 depletion and again, total H3 levels were unaltered (Fig. 5*J*). The H3K27me3 enrichment in the JARID2-depleted cells was below the IgG control signal; therefore, the value was zeroed. We also observed a decrease in EZH2 enrichment on the *Ccne1* promoter upon JARID2 depletion (Fig. 5*K*), showing that JARID2 is required to recruit PRC2

to the *Ccne1* promoter. Together, these data establish that *Ccnd1* and *Ccne1* are direct targets of the PRC2 complex and that JARID2 directs the PRC2 complex to these target genes.

### RB1 is also a direct target of JARID2 and the PRC2 complex

Cyclin D1 and cyclin E1 function to prevent cell cycle exit by inhibiting the function of the RB1. RB1 is required for the irreversible cell cycle exit associated with the arrest of myoblasts and myogenic differentiation (13, 14). We showed that RB1 was down-regulated upon JARID2 depletion (Fig. 3, *A* and *B*), but RB1 has also been shown to cooperate with PRC2 in the methylation of cell cycle genes (13). To understand if *Rb1* itself was a target of H3K27me3, we asked if the *Rb1* gene was a direct target of JARID2 and the PRC2 complex. We found that JARID2 was recruited to the *Rb1* promoter and depletion of JARID2 reduced this association (Fig. 6*A*). We next examined the histone methylation of the *Rb1* promoter. We found that the H3K9 methylation profile was significantly low and was not altered upon JARID2 depletion (Fig. 6*B*), but H3K27 methylation was significantly reduced (Fig. 6*C*). Total H3 was not reduced and, in fact, was modestly enhanced upon JARID2 depletion (Fig. 6*C*). We also examined the association of EZH2 and found that EZH2 was associated with the *Rb1* promoter and the depletion of JARID2 reduced this binding (Fig. 6*D*). Thus, *Rb1* is a direct target of a JARID2-guided PRC2 complex. However, our data clearly show that the relief of H3K27me inhibition is not sufficient to overcome the cyclin D1–mediated repression of *Rb1*.

We next asked if the *Cdkn1a* was directly regulated by JARID2. ChIP assays were performed for JARID2, EZH2, H3K27me3, and H3K9me. However, we did not see any signif-

icant change in the enrichment of H3K9me, H3K27me3, JARID2, and EZH2 for the *Cdkn1a* promoter upon JARID2 depletion (Fig. S3), suggesting that *Cdkn1a* is not a direct target of the JARID2-guided PRC2 complex. We do, however, note that H3K27me3 was enriched on the *Cdkn1A* promoter and this association was lost upon EZH2 depletion, indicating that
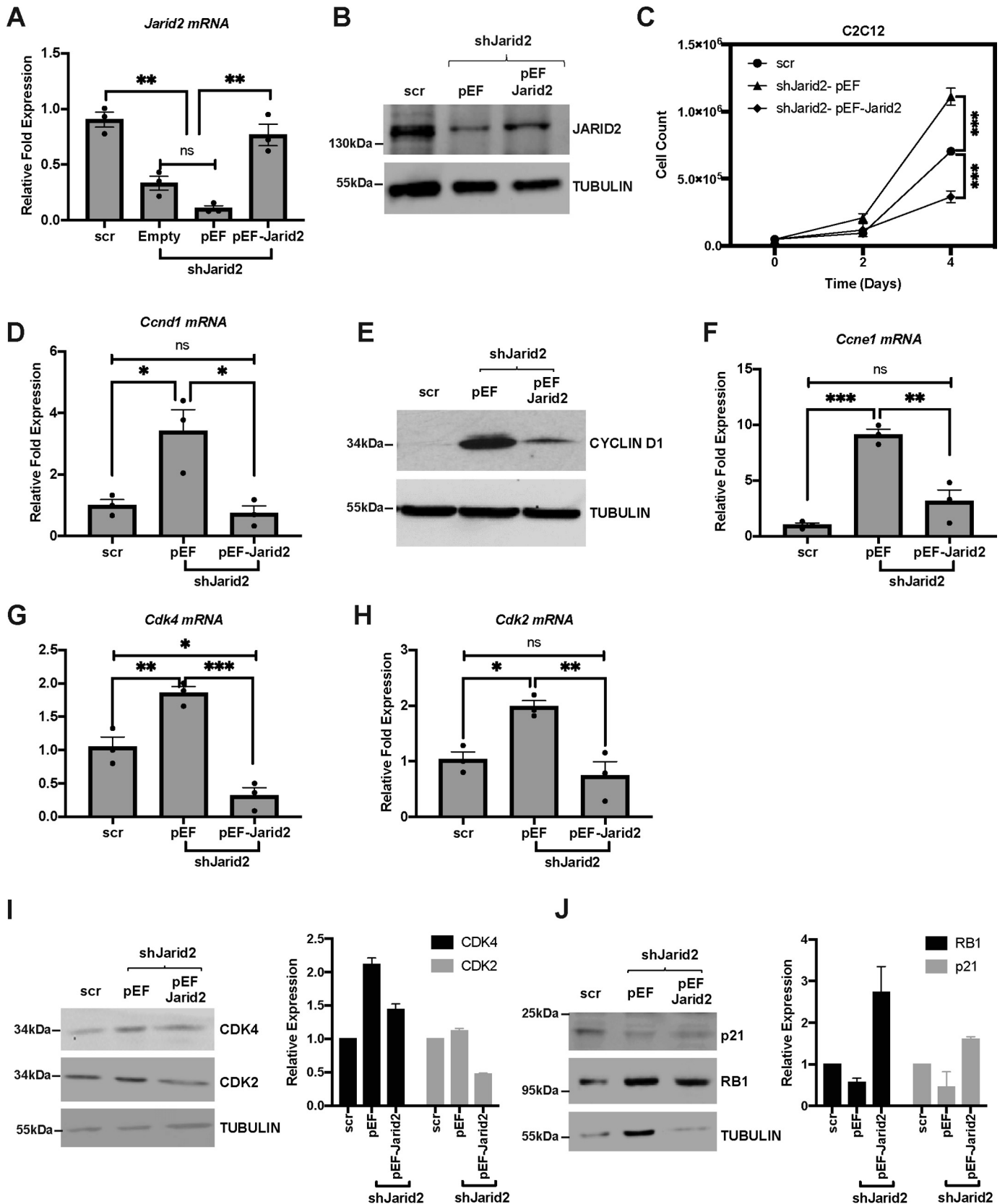
EZH2 does directly regulate the *Cdkn1a* locus.[3] Our results indicate that this regulation may be independent of JARID2.

To understand how the suppression of *Rb1* contributed to the effects observed in JARID2-depleted cells, we used expression construct for RB1-WT and a constitutively active form of RB1 which contains 14 mutated phosphorylation sites (RB-NPC) (34). These constructs were transiently transfected in scr and JARID2-depleted cells. Cells were harvested both before and after differentiation conditions. The known up-regulation of RB1 upon differentiation and the loss of RB1 expression in JARID2-depleted cells could be observed in this experiment (Fig. 6E). We found that RB1-WT could efficiently silence cyclin D1 expression in JARID2-depleted cells (Fig. 6E). The nonphosphorylatable form of RB1 (NPC) did not effectively suppress cyclin D1 (Fig. 6E). Phosphorylation of RB1 releases E2F and our data suggest that phosphorylation of RB1 is required for cyclin D1 repression. We have also shown that the depletion of JARID2 inhibits the expression of myogenin through the loss of β-catenin–mediated expression of MyoD (29). Although RB1 could effectively suppress cyclin D1, it could not restore myogenin expression (Fig. 6E). Thus, the effects of JARID2 on the cell cycle and Wnt pathway signaling are independent and show that JARID2 and the PRC2 complex regulate myogenesis through multiple pathways.

### Transient loss of JARID2 transiently up-regulates cyclin D1

Our results showing that JARID2 is required to restrain proliferation through the PRC2 complex were surprising given that ablation of EZH2 has been shown to lead to reductions in the muscle stem cell pool (35). In our companion manuscript with EZH2,[3] we show that EZH2 restrains cell proliferation through precise regulation of both positive and negative cell cycle genes in skeletal muscle and that the resulting phenotype of enhanced proliferation or cell death correlated to the level of EZH2 depletion or inhibition. To understand if JARID2 had similar effects, we asked if we could observe enhanced proliferation and the up-regulation of cyclin D1 using a transient depletion approach. JARID2 was transiently depleted in C2C12 cells using the same shRNAs used to generate the stable cell lines, and cells were harvested 24 and 48 h following the transfection. Quantification of JARID2 mRNA following the depletion is shown in Fig. 7A. Unlike EZH2 depletion or loss, we did not see any discernible difference in cell proliferation (Fig. 7B). However, we also did not observe enhanced proliferation, indicating that stable depletion of JARID2 is required to see this effect. *Myogenin* is a known target of the PRC2 complex in skeletal muscle (33) and we found that an immediate up-regulation of *Myog* could be observed in the transient approach (Fig. 7C). However, the expression quickly returned to normal levels by

48 h post transfection (Fig. 7C). We next asked how cyclin D1 expression was affected in a transient depletion of JARID2. Like *myogenin*, we saw an immediate burst of mRNA expression 24 h post transfection. However, by 48 h post transfection the expression was lower than the scrambled control (Fig. 7D). At the protein level, no up-regulation of cyclin D1 could be detected (Fig. 7E). To confirm that JARID2 was depleted in this approach, protein expression of JARID2 was examined as well, and we saw that JARID2 was down-regulated, consistent with the mRNA analysis (Fig. 7E). The depletion efficiency of JARID2 correlated closely with the burst of *Ccnd1* mRNA expression detected in this approach.

C2C12 cells are known to have mutated p16/p19 locus (36), and it was not clear what impact the mutated locus had on the results we observed with C2C12 cells. To answer this question, we next used freshly isolated primary myoblasts to determine whether we could recapitulate the results we saw with C2C12 cells. JARID2 was transiently depleted in primary myoblasts using the shRNA constructs used for stable depletion and cells harvested 24 or 48 h post transfection. We found that JARID2 was depleted at both time points (Fig. 8A), but as we saw in C2C12 cells, an up-regulation of cyclin D1 expression could be observed at 24 h post transfection, but cyclin D1 levels quickly returned to baseline 48 h post transfection (Fig. 8B). Again similar to what we observed in C2C12 cells using a transient approach, we observed no changes in cell cycle progression upon on the transient loss of JARID2 in primary myoblasts (Fig. 8C). We also saw no significant increase in DNA synthesis as assayed by an EdU incorporation assay (Fig. 8D). At the 48 h time point, all positive cell cycle genes assayed were down-regulated including *Ccne1* (Fig. 8E), *Cdk4* (Fig. 8F), and *Cdk2* (Fig. 8G). Down-regulation of CYCLIN D1, CDK4, and CDK2 were observed at the protein level as well (Fig. 8H). As we observed with a transient EZH2 depletion,[3] the negative cell cycle regulator *Cdkn1a* (p21) was up-regulated (Fig. 8I), and this effect could also be seen at the protein level (Fig. 8H). The *Cdkn2a* (p16/p19) locus was down-regulated (Fig. 8J), indicating that the loss of this locus is not implicated in the proliferation defect observed in C2C12 cells upon stable depletion of JARID2. Intriguingly, although a significant effect on cell viability was not observed upon transient JARID2 depletion, we did observe increased mRNA expression of the pro-apoptotic gene *Bax* (Fig. 8K) and decreased expression of the anti-apoptotic factor *Bcl2* (Fig. 8L) in primary myoblasts upon transient depletion of JARID2. These mRNA results recapitulate what we saw with transient EZH2 depletion where significant reductions in cell viability were observed.[3]

**Figure 4. JARID2 rescues cell cycle regulator de-repression in JARID2-depleted cells.** *A* and *B*, Scr and shJarid2 C2C12 cells were transfected with empty vector (pEF) or a *Jarid2* (mRNA) expression construct (pEF Jarid2). Cells were assayed by qRT-PCR (*A*) and Western blotting (*B*) for *Jarid2* expression. TUBULIN was used as the loading control. *C*, restoration of JARID2 expression rescues proliferation impairment. An equal number of cells in *A* were assayed for proliferation on indicated time points. *D* and *E*, JARID2 rescues cyclin D1 de-repression. Cells in *A* were assayed for cyclin D1 by qRT-PCR (*D*) and Western blotting assays (*E*). TUBULIN was used as the loading control. *F*, JARID2 rescues cyclin E1 de-repression. Cells in *A* were assayed for cyclin E1 by qRT-PCR. *G* and *H*, cells in *A* were assayed for Cdk4 (*G*) and Cdk2 (*H*) by qRT-PCR. *I*, Western blot analysis of CDK4 and CDK2 in cells on the restoration of JARID2 expression as in *A*. TUBULIN was used as the loading control. The blots were quantified and plotted after normalizing to TUBULIN loading control (*right panel*). *J*, cells in *A* were assayed for negative cell cycle regulators, p21 and RB1, by Western blot analysis. TUBULIN was used as a loading control. The blots were quantified and plotted after normalizing to TUBULIN loading control (*right panel*). *Error bars*, mean ± S.E. (Analysis of variance test followed by Tukey's multiple comparisons test; *ns* represents not significant; *, $p < 0.05$; **, $p < 0.01$; and ***, $p < 0.001$, $n = 3$ biological replicates.)
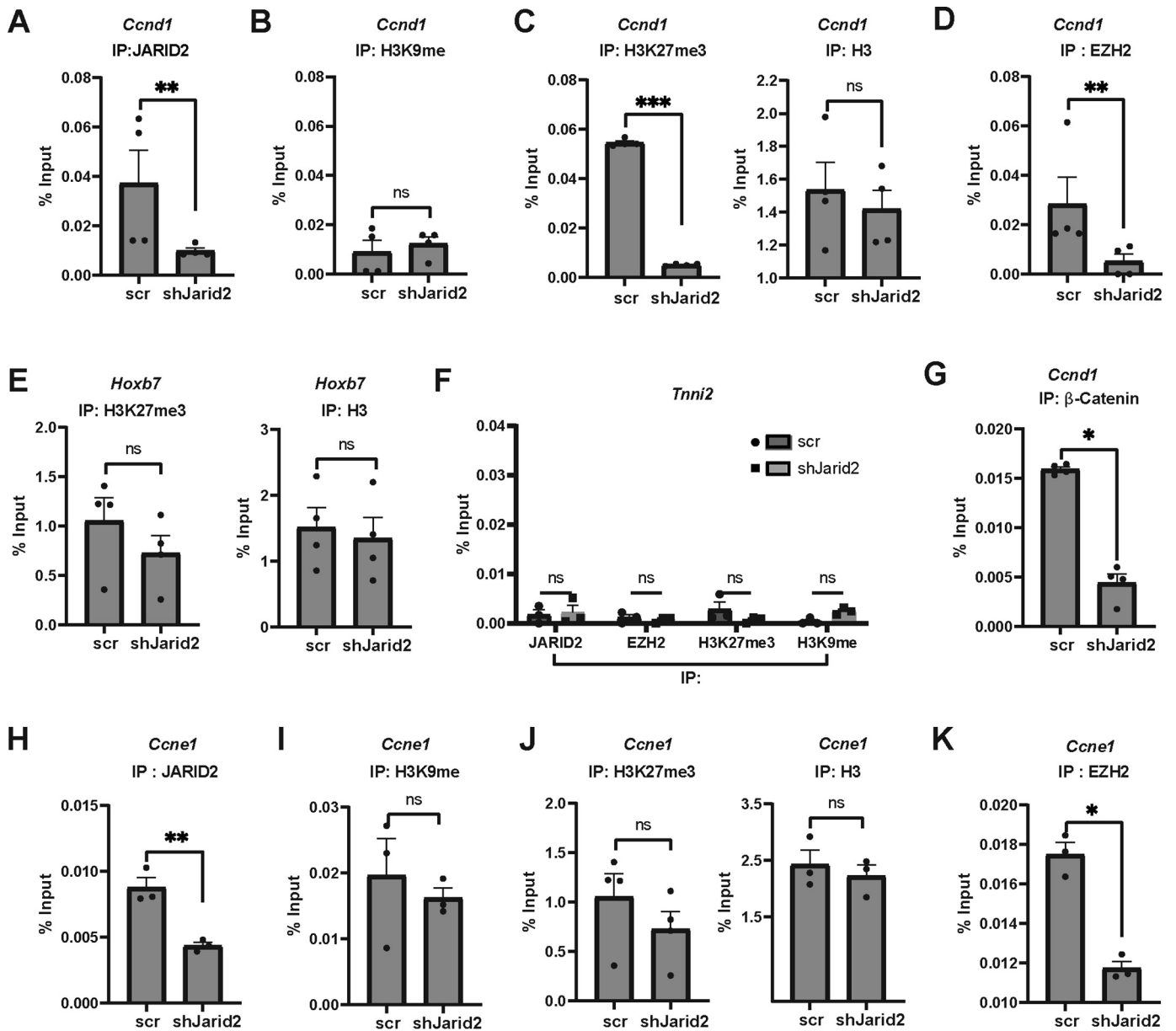
**Figure 5. JARID2 directly regulates the expression of cyclin D1 and cyclin E1 via PRC2 recruitment.** *A–D*, ChIP assays were performed on proliferating scr and JARID2-depleted (shJarid2) C2C12 cells with antibodies against JARID2 (*A*), H3K9me (*B*), H3K27me3 and H3 (*C*), EZH2 (*D*), and primers spanning the *Ccnd1* promoter. *E*, cells in *A* were assayed for H3K27me3 and H3 status on a *HoxB7* region as a positive control. *F*, cells in *A* were assayed for the JARID2, EZH2, H3K27me3, and H3K9me status on *Tnni2* proximal promoter as a negative control. *G*, β-catenin recruitment is not enhanced in JARID2-depleted cells. ChIP assay on cells as in *A* with antibodies against β-catenin and primers spanning the *Ccnd1* promoter. *H–K*, JARID2 also directly regulates cyclin E1 (*Ccne1*) through PRC2 recruitment. ChIP assays were performed on cells as in *A* with antibodies against JARID2 (*H*), H3K9me (*I*), H3K27me3 and H3 (*J*), EZH2 (*K*), and primers spanning the *Ccne1* promoter. IgG background signals were subtracted from IP signals. *Error bars*, mean ± S.E. (Student's *t* test; *ns* represents not significant; *, $p < 0.05$; **, $p < 0.01$; and ***, *p* value $< 0.001$; $n = 3$–4 biological replicates.)

Together, our results confirm that JARID2 directly regulates cyclin D1 through the PRC2 complex, but because of the complex effects on both positive and negative cell cycle genes, sustained depletion is required to see a sustained activation of cyclin D1 and enhanced proliferation.

## Discussion

In this work, we show that JARID2, along with the PRC2 complex, restrains proliferation by repressing the pro-proliferative cell cycle regulators cyclin D1 and cyclin E1. When expressed, these factors then phosphorylate RB1, thus releasing

activator E2F transcription factors that further up-regulate various cell cycle genes including cyclin E1. This feed-forward loop forms a switch that decides whether the cell proceeds to S phase surpassing the $G_1$/S restriction point or exits the cell cycle in a RB1-dependent manner.

Our finding that JARID2 regulates cell proliferation is in agreement with the previous finding in heart muscle which showed that JARID2 regulates cell proliferation through repression of the *Ccnd1* gene (25, 27). However, unlike in cardiomyocytes where JARID2 has been shown repress *Ccnd1* by H3K9 methyltransferases (30), we show that JARID2 represses
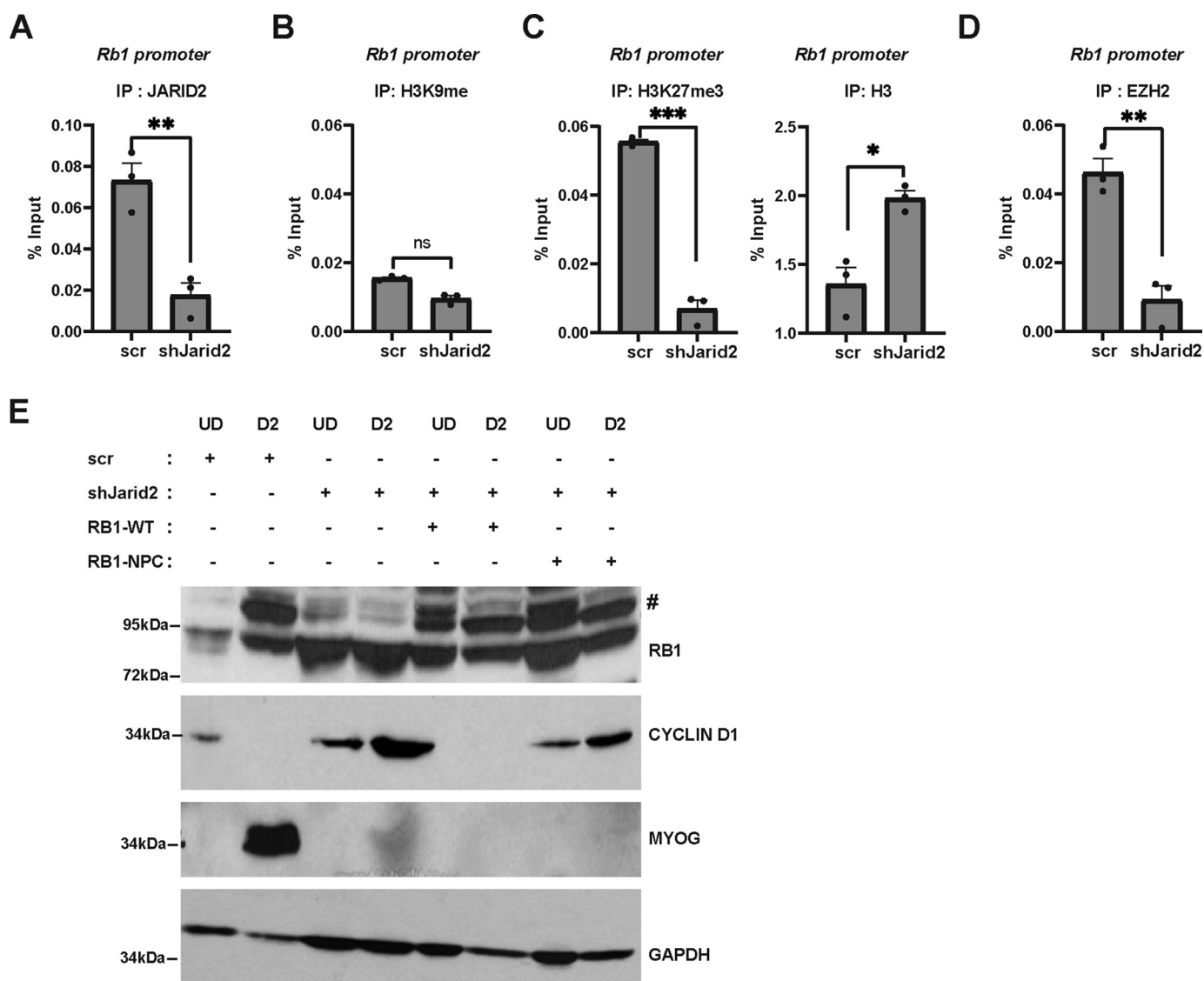
**Figure 6. Rb1 is directly regulated by JARID2 but not *Cdkn1a* (p21).** *A–D*, *RB1* is a direct target of JARID2 and the PRC2 complex. ChIP assays were performed on proliferating scr and JARID2-depleted (shJarid2) C2C12 cells with antibodies against JARID2 (*A*), H3K9me (*B*), H3K27me3 and H3 (*C*) EZH2 (*D*), and primers spanning the *Rb1* promoter. IgG background signals were subtracted from immunoprecipitation signals. *E*, restoration of RB1 can inhibit cyclin D1, but not activate myogenin. C2C12 cells with scrambled (scr) and JARID2 depletion (shJarid2) were transiently transfected with expression constructs for RB1 (RB1-WT), and RB1 mutated at phosphorylation sites (RB1-NPC). *UD* represents the proliferative, undifferentiated time point and *D2'* represents 2 days in differentiation media. Cells were analyzed for total RB1, cyclin D1, and myogenin. GAPDH was used as a loading control. # represents the band of interest for RB1 protein as determined by molecular weight standards. *Error bars*, mean ± S.E. (Student's *t* test; *ns* represents not significant, *, $p$ value < 0.05; **, $p$ value < 0.01; ***, $p$ value < 0.001; $n$ = 3 biological replicates.)

*Ccnd1* by recruiting a H3K27 methyltransferase, the PRC2 complex, in skeletal muscle. This finding is in agreement with previous findings that showed no significant contribution of H3K9 methylation during skeletal muscle differentiation (33). JARID2 has also been shown to regulate various target genes in a PRC2-dependent manner during cardiac development as well (38). Clearly, the role of JARID2, an inactive histone demethylase, and its regulatory partner complexes is evolutionarily diverse depending on cell type. It is interesting that JARID2/PRC2 directly regulates both cyclin D1 and cyclin E1 to maintain control of the cell cycle. The dual regulation serves to maintain control of two central regulators of the $G_1$/S transition phase. Our results also suggest that the PRC2 complex has many divergent roles in

skeletal muscle cells that require a fine balance of JARID2 and EZH2 expression.

Intriguingly, JARID2 and the PRC2 complex also methylate *Rb1* in proliferating cells, the repression of which prevents mitotic exit and terminal differentiation. Thus, the normal function of JARID2 and the PRC2 complex in skeletal muscle appears to be restraining the rate of proliferation while also preventing mitotic exit. In the JARID2 depletions characterized here, the loss of inhibition of cyclin D1 dominates the potential de-repression of *Rb1.* However, when JARID2 expression was restored, it was interesting that the normal expression of both negative and positive cell cycle regulators was restored. In this case, the repression of *cyclin D1* is clearly sufficient to restore RB1 expression, irrespective of H3K27 methylation.
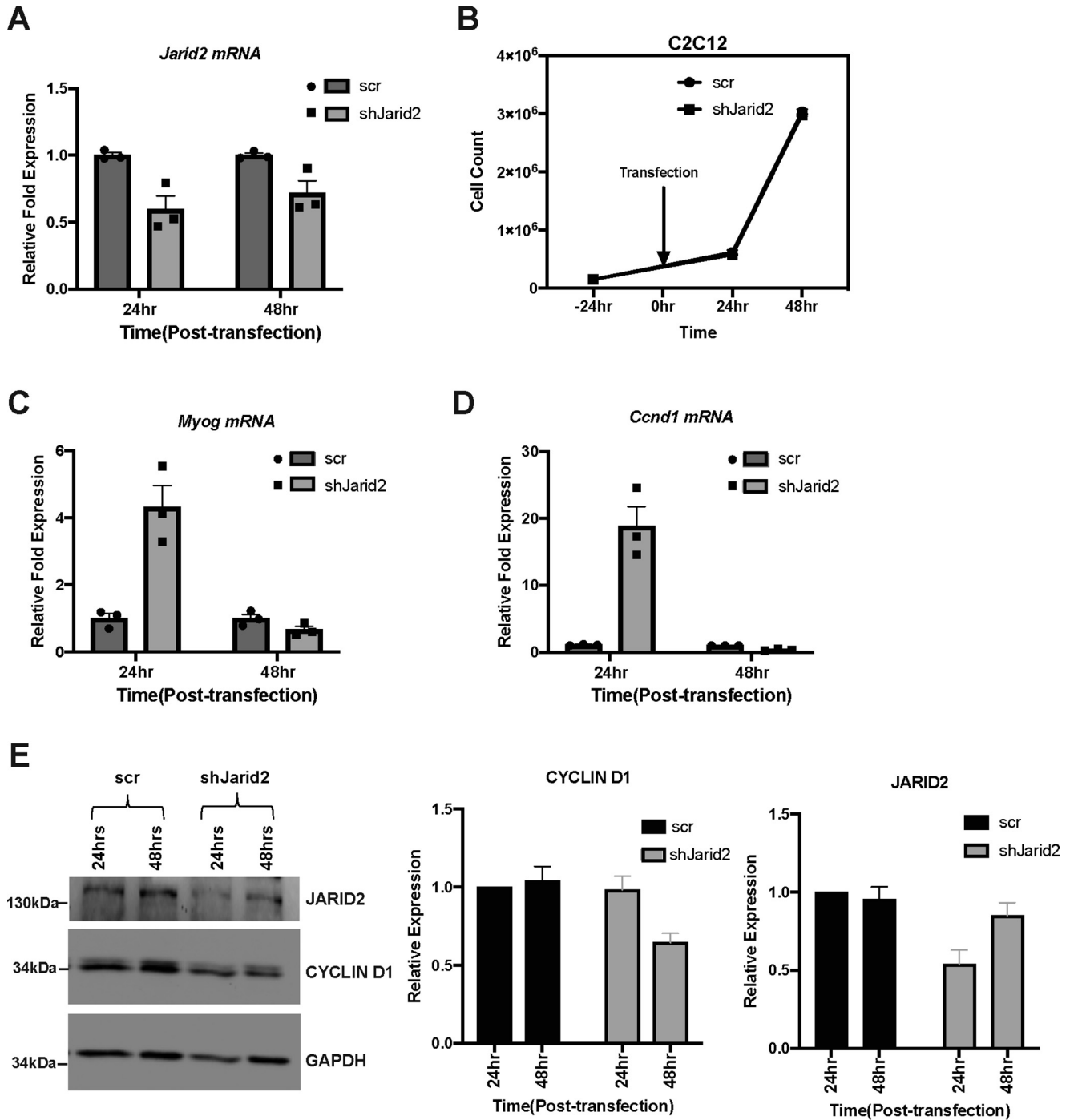
**Figure 7. Transient loss of Jarid2 does not decrease cell viability in C2C12 cells.** *A,* C2C12 cells were transiently transfected with scrambled (scr) or shRNA against Jarid2 (shJarid2) without drug selection and were analyzed for JARID2 expression by qRT-PCR at indicated time point post transfection. *B,* cells in *A,* were assayed for proliferation rate. *C,* JARID2 regulates myogenin in C2C12 cells. Cells in *A* were assayed for myogenin expression by qRT-PCR. *D* and *E,* cyclin D1 is regulated by JARID2. *D,* cells in *A* were assayed for cyclin D1 expression by qRT-PCR. *E, left panel,* cells in *A* were assayed for CYCLIN D1 and JARID2 expression by Western blotting. GAPDH was used as a loading control. *E, right panel,* blots were quantified and normalized to GAPDH and plotted. *Error bars,* mean ± S.E. (*n* = 3 biological replicates.)

JARID2 has also been shown to regulate cell proliferation through repression of *Ccnd1* in leukemia (28). JARID2 has been identified as an oncogene that is often overexpressed in multiple cancers including rhabdomyosarcoma (39). In rhabdomyosarcoma, JARID2 is essential for cell viability and loss of JARID2 rescues partial differentiation in rhabdomyosarcoma (39). However, JARID2 has recently been shown to act as tumor suppressor in myeloid neoplasm through restriction of hematopoietic progenitor cells self-renewal (40).

Importantly, in our study we found that JARID2 could be efficiently depleted in C2C12 cells without a significant impact on viability, unlike EZH2. We did observe changes in apoptotic cell marker expression upon transient JARID2 depletion in primary myoblasts, so it remains to be determined if JARID2 could
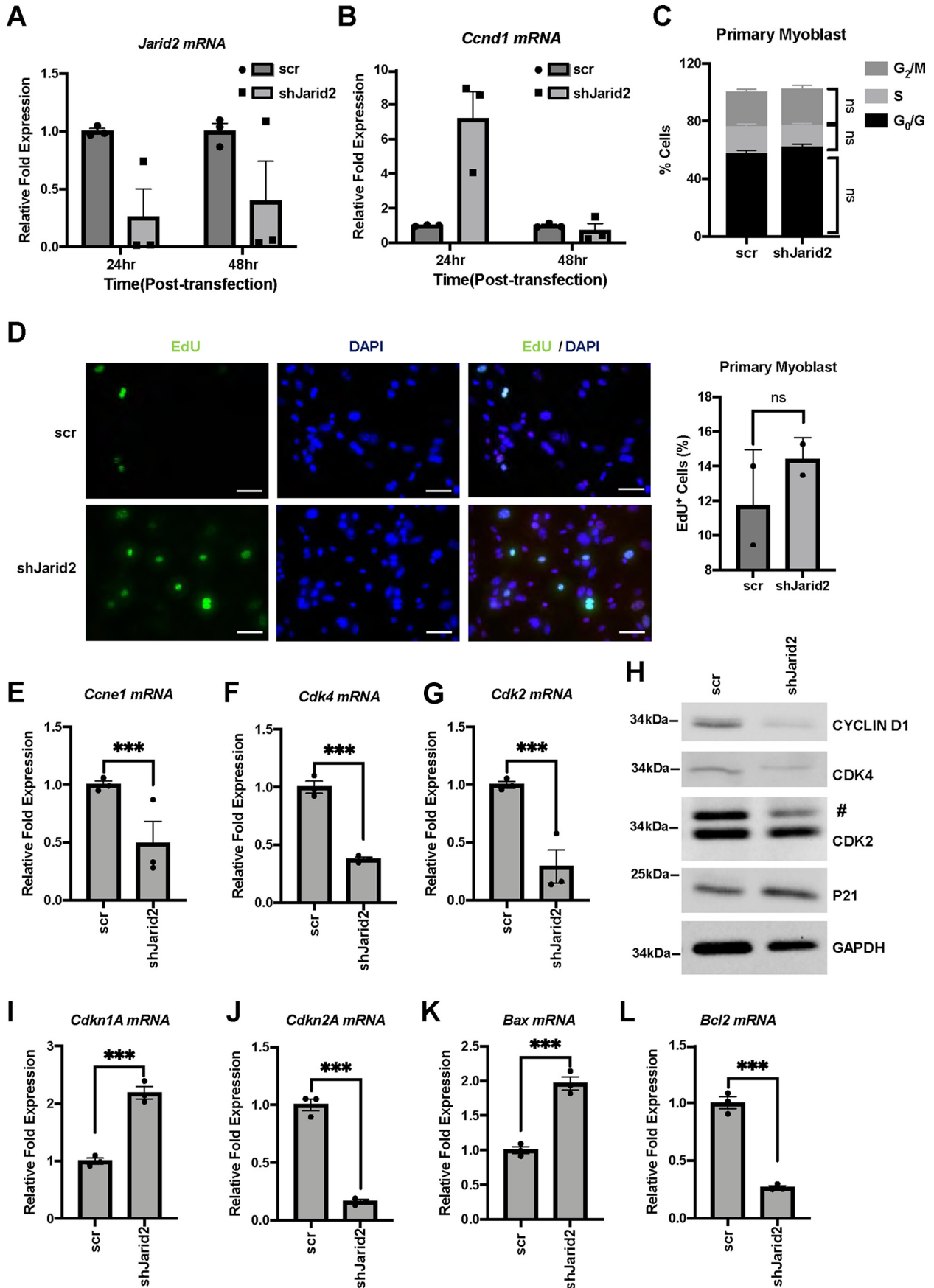
be deleted in primary cells without an impact on viability. Recent studies have shown that the expression Cdk4/cyclin D1 expands neural stem cells and increases neurogenesis (41). It has also been shown that regulation of the cell cycle through reintroduction of cyclin D1 and CDK4 in cardiac cells can increase cardiac cell regeneration and repair post injury (42). Our work suggests that inhibiting the function of JARID2 could potentially be used to expand the muscle stem cell pool and enhance muscle repair and regeneration. Clearly, the roles of JARID2 and the PRC2 complex are complex in skeletal muscle and serve to both inhibit and activate several steps of the myogenic program. Characterization of each of these roles aid in the understanding of how these factors are involved in normal myogenesis, repair, and disease.

## Experimental procedures

### Cell culture

C2C12 cells (ATCC) were grown in DMEM, supplemented with 10% FBS (HyClone Laboratories) according to standard protocols. Proliferating C2C12 myoblasts were grown in DMEM supplemented with 10% FBS (HyClone Laboratories), and 2% horse serum (Gibco Laboratories) in DMEM was used to induce differentiation. Primary myoblasts were isolated according to standard protocols (43). Briefly, hind limb muscles of neonatal mice were isolated and digested with Collagenase Type II (Worthington Biochemical Corp.). Cells were filtered through a sterile 70-micron filter, plated on gelatin-coated plates in 20% FBS in F-10 basal media with $1\times$ penicillin-streptomycin (Corning) and 2.5 ng/ml bFGF (gift of D. Cornelison, University of Missouri). Primary myoblasts were enriched by pre-plating cells onto uncoated plates for 30 min before transferring myoblast suspensions to collagen-coated plates and repeating until the majority of the cells were myoblasts. Myoblast identity was confirmed by expression analysis of MRFs, differentiation assays, and myosin heavy chain immunofluorescence. All mouse procedures were approved by the Southern Illinois University Institutional Animal Care and Use Committee.

### Plasmid constructs

JARID2 was depleted with shRNA constructs designed by the RNAi Consortium in the pLOK.1 plasmid (Open Biosystems) as described (29). Three constructs targeting murine Jarid2 and one scrambled control were linearized using the ScaI restriction enzyme (New England Biolabs), transfected into C2C12 cells using TurboFect (Thermo Scientific) following manufacturer's protocol, and selected with puromycin (2 $\mu$g/ml). Individual clones were selected, propagated, and confirmed by mRNA and protein analysis. For transient transfections, circular (uncut) plasmids were transfected using TurboFect. mRNA and protein were extracted at indicated time points. Drug selection was not used for transient transfection experiments.

The coding sequence of murine *Jarid2* was PCR amplified from cDNA reverse transcribed from the total RNA extracted from proliferating C2C12 cells. The PCR amplified *Jarid2* insert was cloned into the pEF6/V5 His TOPO TA expression vector according to manufacturer's protocol (Invitrogen). The clones were confirmed by sequencing. For rescue of JARID2 expression, pEF6-Jarid2 plasmid was stably transfected in C2C12 cells previously depleted of JARID2 using shRNA construct (mature antisense sequence: 5′-AAATTGCACATGGATGACAGG-3′) that targets 3′-untranslated region (UTR) of *Jarid2* mRNA. The stable clones were selected with blasticidin (10 $\mu$g/ml), confirmed by mRNA and protein analysis.

Expression plasmids for WT and a nonphosphorylatable form (NPC) of retinoblastoma protein (RB1) were generated in the lab of Sibylle Mittnacht (University College London Cancer Institute) (34). Colin Goding (University of Oxford Ludwig Cancer Research) used these constructs to characterize the interaction of Mitf and RB1 (37) and generously gifted these constructs to our laboratory. The constructs were confirmed by restriction enzyme mapping and sequencing. The plasmids were transfected using TurboFect as described previously.

### Western blot analysis

Cell extracts were made by lysing PBS washed cell pellets in radioimmune precipitation assay buffer (RIPA) supplemented with protease inhibitors (cOmplete Protease Inhibitor, Roche Diagnostics). Following incubation on ice, clear lysates were obtained by centrifugation. Protein concentrations were determined by Bradford's assay (Bio-Rad). For each sample, 30 $\mu$g of protein was loaded on each gel unless otherwise specified. Proteins were transferred onto a PVDF membrane using a tank blotter (Bio-Rad). The membranes were then blocked with 5% milk in $1\times$ Tris-buffered saline plus Tween 20 (TBST) and incubated with primary antibody overnight at 4 °C. Membranes were then washed with $1\times$ TBST and incubated with the corresponding secondary antibody. Membranes were again washed with $1\times$ TBST, incubated with chemiluminescent substrate according to manufacturer's protocol (SuperSignal, Pierce) and visualized by an iBright Imaging System or developed by autoradiography. The antibodies used include anti-JARID2 (ABclonal), anti-cyclinD1 (DCS-6, Invitrogen), anti-cyclin E1 (Santa Cruz Biotechnology), anti-CDK2 (ABclonal), anti-CDK4 (ABclonal), anti-pRB1 (LabVision) (Fig. 4I), anti-pRB1(Cell Signaling Technology) (Figs. 3B and 6E), anti-p21 (ABclonal), anti-tubulin (E7, Developmental Studies Hybridoma

**Figure 8. Transient loss of Jarid2 does not decrease cell viability in primary myoblasts.** *A*, freshly isolated primary myoblasts were transiently transfected with scrambled (scr) control or shRNA against Jarid2 (shJarid2) without drug selection. Jarid2 expression was assayed by qRT-PCR at the indicated time points. *B*, cells in *A* were assayed for cyclin D1 expression by qRT-PCR. *C*, transient loss of Jarid2 in primary myoblast does not have significant change cell cycle progression. Cells in *A* were ethanol fixed, propidium iodide stained, and analyzed for cell cycle phase distribution using flow cytometry. *D*, transient loss of Jarid2 did not result in a significant increase in DNA synthesis in primary myoblasts. Cells in *A* were assayed for DNA synthesis by EdU incorporation assay (*left panel*). Five random fields were counted for EdU$^+$ nuclei and plotted (*right panel*). DAPI was used to stain nuclei. *Scale bar*, 50 $\mu$m; *n* = 2 biological replicates. *E–J*, cell cycle genes are deregulated upon transient loss of Jarid2 in primary myoblasts. Cells as in *A* were analyzed for the expression of cyclin E1 (*Ccne1*) (*E*), *Cdk4* (*F*), *Cdk2* (*G*), p21 (*Cdkn1a*) (*I*), and *Cdkn2a* (p16/19) (*J*) by qRT-PCR and Western blotting (*H*). GAPDH was used as a loading control. **#** represents the band of interest for CDK2 based on molecular weight standards. *K* and *L*, Jarid2 depletion increased apoptotic marker expression in primary myoblasts. Cells in *A* were assayed for the pro-apoptotic marker *Bax* (*K*) and anti-apoptotic marker *Bcl2* (*L*) by qRT-PCR. *Error bars*, mean $\pm$ S.E. (Student's *t* test; *ns* represents not significant; ***, $p < 0.001$; *n* = 3 biological replicates.)

Bank), and anti-GAPDH (Millipore). Protein expression levels were quantified using iBright analysis software or ImageJ (National Institutes of Health) software on at least three independent experiments unless otherwise mentioned. Representative images are shown.

### Quantitative real-time PCR

RNA was isolated from cells by TRIzol extractions (Invitrogen). Following treatment with DNase (Promega), 2 $\mu$g of total RNA was reversed transcribed with MultiScribe™ MuLV Reverse Transcriptase (Applied Biosystems). cDNA equivalent to 40 ng was used for quantitative PCR amplification (Applied Biosystems) with SYBR green PCR master mix (Applied Biosystems). Samples in which no reverse transcriptase was added (no RT) were included for each RNA sample. Quantitative PCR data were calculated using the comparative *Ct* method (Applied Biosystems). Standard deviations from the mean of the [$\Delta$] *Ct* values were calculated from three independent RNA samples. Primers are described in Table S1. Where possible, intron-spanning primers were used. All quantitative PCR was performed in triplicate, and three independent RNA samples were assayed for each time point. For measurements of relative gene expression, a -fold change was calculated for each sample pair and then normalized to the -fold change observed at hypoxanthine guanine phosphoribosyl transferase (HPRT) and/or 18S rRNA.

### ChIP assays

ChIP assays were performed as described previously (37). The following antibodies were used: anti-Jarid2 (Cell Signaling Technology), anti-Ezh2 (Cell Signaling Technology), anti-H3K27me3 (Cell Signaling Technology), anti-H3K9me (pan) (Cell Signaling Technology), anti-H3 (Cell Signaling Technology) and anti-$\beta$-Catenin (Santa Cruz Biotechnology). Rabbit IgG (Santa Cruz Biotechnology) was used as a nonspecific control. Primers are described in Table S1. The real-time PCR was performed in triplicate. The results were represented as the percentage of immunoprecipitation over input signal (% Input) with IgG background signal subtracted. All ChIP assays shown are representative of at least three individual experiments unless otherwise stated. Standard error from the mean was calculated and plotted as the error bar.

### EdU incorporation assay

Cells were assayed using a Click-iT EdU Alexa Fluor 488 Imaging Kit according to the manufacturer's protocol (Life Technologies). C2C12 and primary myoblast cells were grown in the presence of EdU for 2 and 3 h, respectively. EdU positive nuclei were counted in at least five random fields on microscopic images taken at 200$\times$ and 400$\times$ magnification using a Leica microscope.

### Proliferation assay

An equal number of cells were seeded, and on the indicated days, cells were harvested using trypsin, resuspended and counted under a light microscope using a hemocytometer. Cell viability was determined by Trypan Blue staining. Cell counting was performed in duplicate for at least three blinded biological replicates.

### Cell cycle analysis by flow cytometry

Cells were split in 100-mm diameter plates at 1:5 dilution, grown for 48 h in duplicates in 10% FBS in 5% $CO_2$ incubator. The cell plates were washed twice with sterile 1$\times$ PBS, pH 7.4, harvested using trypsin, and resuspended in 1$\times$ PBS, pH 7.4. Cells were pelleted down at 600 $\times$ *g* for 5 min at room temperature, washed twice with 1$\times$ PBS and were fixed in chilled 70% ethanol overnight at $-20$ °C. Cells were washed with 1$\times$ PBS, pH 7.4, treated with RNase (10 $\mu$g/ml), and stained with propidium iodide (50 $\mu$g/ml) for 2 h at room temperature before running through a BD Accuri C6 flow cytometer (BD Biosciences). Data were analyzed using FlowJo (FlowJo LLC) software.

### Statistics

Data are presented as mean $\pm$ S.E. Statistical comparisons were performed using the unpaired two-tailed Student's *t* tests and analysis of variance (ANOVA) test followed by Tukey's multiple comparison test. A probability value of $< 0.05$ was taken to indicate significance. All statistical analyses and graphs were made in GraphPad Prism 8.0 software.

### References

1. Shen, X., Collier, J. M., Hlaing, M., Zhang, L., Delshad, E. H., Bristow, J., and Bernstein, H. S. (2003) Genome-wide examination of myoblast cell cycle withdrawal during differentiation. *Dev. Dyn.* **226,** 128–138 CrossRef Medline
2. Geng, Y., Yu, Q., Sicinska, E., Das, M., Bronson, R. T., and Sicinski, P. (2001) Deletion of the p27Kip1 gene restores normal development in cyclin D1-deficient mice. *Proc. Natl. Acad. Sci. U.S.A.* **98,** 194–199 CrossRef Medline
3. Hitomi, M., and Stacey, D. W. (1999) Cyclin D1 production in cycling cells depends on ras in a cell-cycle-specific manner. *Curr. Biol.* **9,** 1075–1084 CrossRef Medline
4. Berkes, C. A., and Tapscott, S. J. (2005) MyoD and the transcriptional control of myogenesis. *Semin. Cell Dev. Biol.* **16,** 585–595 CrossRef Medline
5. Lassar, A. B., Skapek, S. X., and Novitch, B. (1994) Regulatory mechanisms that coordinate skeletal muscle differentiation and cell cycle withdrawal. *Curr. Opin. Cell Biol.* **6,** 788–794 CrossRef Medline
6. Molkentin, J. D., and Olson, E. N. (1996) Combinatorial control of muscle development by basic helix-loop-helix and MADS-box transcription factors. *Proc. Natl. Acad. Sci. U.S.A.* **93,** 9366–9373 CrossRef Medline
7. Liu, Q. C., Zha, X. H., Faralli, H., Yin, H., Louis-Jeune, C., Perdiguero, E., Pranckeviciene, E., Muñoz-Cànoves, P., Rudnicki, M. A., Brand, M., Perez-Iratxeta, C., and Dilworth, F. J. (2012) Comparative expression profiling identifies differential roles for myogenin and p38$\alpha$ MAPK signaling in myogenesis. *J. Mol. Cell Biol.* **4,** 386–397 CrossRef Medline
8. Guo, K., Wang, J., Andrés, V., Smith, R. C., and Walsh, K. (1995) MyoD-induced expression of p21 inhibits cyclin-dependent kinase activity upon myocyte terminal differentiation. *Mol. Cell. Biol.* **15,** 3823–3829 CrossRef Medline

ASBMB

*J. Biol. Chem.* (2019) 294(51) 19451–19464 **19463**

9. Halevy, O., Novitch, B. G., Spicer, D. B., Skapek, S. X., Rhee, J., Hannon, G. J., Beach, D., and Lassar, A. B. (1995) Correlation of terminal cell cycle arrest of skeletal muscle with induction of p21 by MyoD. *Science* **267,** 1018–1021 CrossRef Medline

10. Sherr, C. J., and Roberts, J. M. (1999) CDK inhibitors: Positive and negative regulators of G$_1$-phase progression. *Genes Dev.* **13,** 1501–1512 CrossRef Medline

11. Martelli, F., Cenciarelli, C., Santarelli, G., Polikar, B., Felsani, A., and Caruso, M. (1994) MyoD induces retinoblastoma gene expression during myogenic differentiation. *Oncogene* **9,** 3579–3590 Medline

12. Macaluso, M., Montanari, M., and Giordano, A. (2006) Rb family proteins as modulators of gene expression and new aspects regarding the interaction with chromatin remodeling enzymes. *Oncogene* **25,** 5263–5267 CrossRef Medline

13. Blais, A., van Oevelen, C. J., Margueron, R., Acosta-Alvear, D., and Dynlacht, B. D. (2007) Retinoblastoma tumor suppressor protein-dependent methylation of histone H3 lysine 27 is associated with irreversible cell cycle exit. *J. Cell Biol.* **179,** 1399–1412 CrossRef Medline

14. Huh, M. S., Parker, M. H., Scimè, A., Parks, R., and Rudnicki, M. A. (2004) Rb is required for progression through myogenic differentiation but not maintenance of terminal differentiation. *J. Cell Biol.* **166,** 865–876 CrossRef Medline

15. Narasimha, A. M., Kaulich, M., Shapiro, G. S., Choi, Y. J., Sicinski, P., and Dowdy, S. F. (2014) Cyclin D activates the Rb tumor suppressor by monophosphorylation. *Elife* **3,** e02872 CrossRef Medline

16. Bracken, A. P., Ciro, M., Cocito, A., and Helin, K. (2004) E2F target genes: Unraveling the biology. *Trends Biochem. Sci.* **29,** 409–417 CrossRef Medline

17. Cao, R., Tsukada, Y., and Zhang, Y. (2005) Role of Bmi-1 and Ring1A in H2A ubiquitylation and Hox gene silencing. *Mol. Cell* **20,** 845–854 CrossRef Medline

18. Cao, R., Wang, L., Wang, H., Xia, L., Erdjument-Bromage, H., Tempst, P., Jones, R. S., and Zhang, Y. (2002) Role of histone H3 lysine 27 methylation in Polycomb-group silencing. *Science* **298,** 1039–1043 CrossRef Medline

19. Kuzmichev, A., Nishioka, K., Erdjument-Bromage, H., Tempst, P., and Reinberg, D. (2002) Histone methyltransferase activity associated with a human multiprotein complex containing the Enhancer of Zeste protein. *Genes Dev.* **16,** 2893–2905 CrossRef Medline

20. Müller, J., Hart, C. M., Francis, N. J., Vargas, M. L., Sengupta, A., Wild, B., Miller, E. L., O'Connor, M. B., Kingston, R. E., and Simon, J. A. (2002) Histone methyltransferase activity of a *Drosophila* Polycomb group repressor complex. *Cell* **111,** 197–208 CrossRef Medline

21. Conerly, M. L., MacQuarrie, K. L., Fong, A. P., Yao, Z., and Tapscott, S. J. (2011) Polycomb-mediated repression during terminal differentiation: What don't you want to be when you grow up? *Genes Dev.* **25,** 997–1003 CrossRef Medline

22. Klose, R. J., Kallin, E. M., and Zhang, Y. (2006) JmjC-domain-containing proteins and histone demethylation. *Nat. Rev. Genet.* **7,** 715–727 CrossRef Medline

23. Landeira, D., and Fisher, A. G. (2011) Inactive yet indispensable: The tale of Jarid2. *Trends Cell Biol.* **21,** 74–80 CrossRef Medline

24. Landeira, D., Sauer, S., Poot, R., Dvorkina, M., Mazzarella, L., Jørgensen, H. F., Pereira, C. F., Leleu, M., Piccolo, F. M., Spivakov, M., Brookes, E., Pombo, A., Fisher, C., Skarnes, W. C., Snoek, T., *et al.* (2010) Jarid2 is a PRC2 component in embryonic stem cells required for multi-lineage differentiation and recruitment of PRC1 and RNA polymerase II to developmental regulators. *Nat. Cell Biol.* **12,** 618–624 CrossRef Medline

25. Nakajima, K., Inagawa, M., Uchida, C., Okada, K., Tane, S., Kojima, M., Kubota, M., Noda, M., Ogawa, S., Shirato, H., Sato, M., Suzuki-Migishima, R., Hino, T., Satoh, Y., Kitagawa, M., and Takeuchi, T. (2011) Coordinated regulation of differentiation and proliferation of embryonic cardiomyocytes by a jumonji (Jarid2)-cyclin D1 pathway. *Development* **138,** 1771–1782 CrossRef Medline

26. Takahashi, M., Kojima, M., Nakajima, K., Suzuki-Migishima, R., Motegi, Y., Yokoyama, M., and Takeuchi, T. (2004) Cardiac abnormalities cause early lethality of *jumonji* mutant mice. *Biochem. Biophys. Res. Commun.* **324,** 1319–1323 CrossRef Medline

27. Toyoda, M., Shirato, H., Nakajima, K., Kojima, M., Takahashi, M., Kubota, M., Suzuki-Migishima, R., Motegi, Y., Yokoyama, M., and Takeuchi, T. (2003) *jumonji* downregulates cardiac cell proliferation by repressing *cyclin D1* expression. *Dev. Cell* **5,** 85–97 CrossRef Medline

28. Su, C. L., Deng, T. R., Shang, Z., and Xiao, Y. (2015) JARID2 inhibits leukemia cell proliferation by regulating CCND1 expression. *Int. J. Hematol.* **102,** 76–85 CrossRef Medline

29. Adhikari, A., and Davie, J. (2018) JARID2 and the PRC2 complex regulate skeletal muscle differentiation through regulation of canonical Wnt signaling. *Epigenetics Chromatin* **11,** 46 CrossRef Medline

30. Shirato, H., Ogawa, S., Nakajima, K., Inagawa, M., Kojima, M., Tachibana, M., Shinkai, Y., and Takeuchi, T. (2009) A jumonji (Jarid2) protein complex represses *cyclin D1* expression by methylation of histone H3-K9. *J. Biol. Chem.* **284,** 733–739 CrossRef Medline

31. Pasini, D., Cloos, P. A., Walfridsson, J., Olsson, L., Bukowski, J. P., Johansen, J. V., Bak, M., Tommerup, N., Rappsilber, J., and Helin, K. (2010) JARID2 regulates binding of the Polycomb repressive complex 2 to target genes in ES cells. *Nature* **464,** 306–310 CrossRef Medline

32. Londhe, P., and Davie, J. K. (2013) Interferon-γ resets muscle cell fate by stimulating the sequential recruitment of JARID2 and PRC2 to promoters to repress myogenesis. *Sci. Signal.* **6,** ra107 CrossRef Medline

33. Asp, P., Blum, R., Vethantham, V., Parisi, F., Micsinai, M., Cheng, J., Bowman, C., Kluger, Y., and Dynlacht, B. D. (2011) Genome-wide remodeling of the epigenetic landscape during myogenic differentiation. *Proc. Natl. Acad. Sci. U.S.A.* **108,** E149–E158 CrossRef Medline

34. Chew, Y. P., Ellis, M., Wilkie, S., and Mittnacht, S. (1998) pRB phosphorylation mutants reveal role of pRB in regulating S phase completion by a mechanism independent of E2F. *Oncogene* **17,** 2177–2186 CrossRef Medline

35. Juan, A. H., Derfoul, A., Feng, X., Ryall, J. G., Dell'Orso, S., Pasut, A., Zare, H., Simone, J. M., Rudnicki, M. A., and Sartorelli, V. (2011) Polycomb EZH2 controls self-renewal and safeguards the transcriptional identity of skeletal muscle stem cells. *Genes Dev.* **25,** 789–794 CrossRef Medline

36. Pajcini, K. V., Corbel, S. Y., Sage, J., Pomerantz, J. H., and Blau, H. M. (2010) Transient inactivation of Rb and ARF yields regenerative cells from postmitotic mammalian muscle. *Cell Stem Cell* **7,** 198–213 CrossRef Medline

37. Londhe, P., and Davie, J. K. (2011) Sequential association of myogenic regulatory factors and E proteins at muscle-specific genes. *Skelet. Muscle* **1,** 14 CrossRef Medline

38. Cho, E., Mysliwiec, M. R., Carlson, C. D., Ansari, A., Schwartz, R. J., and Lee, Y. (2018) Cardiac-specific developmental and epigenetic functions of Jarid2 during embryonic development. *J. Biol. Chem.* **293,** 11659–11673 CrossRef Medline

39. Walters, Z. S., Villarejo-Balcells, B., Olmos, D., Buist, T. W., Missiaglia, E., Allen, R., Al-Lazikani, B., Garrett, M. D., Blagg, J., and Shipley, J. (2014) JARID2 is a direct target of the PAX3-FOXO1 fusion protein and inhibits myogenic differentiation of rhabdomyosarcoma cells. *Oncogene* **33,** 1148–1157 CrossRef Medline

40. Celik, H., Koh, W. K., Kramer, A. C., Ostrander, E. L., Mallaney, C., Fisher, D. A. C., Xiang, J., Wilson, W. C., Martens, A., Kothari, A., Fishberger, G., Tycksen, E., Karpova, D., Duncavage, E. J., Lee, Y., Oh, S. T., and Challen, G. A. (2018) JARID2 functions as a tumor suppressor in myeloid neoplasms by repressing self-renewal in hematopoietic progenitor cells. *Cancer Cell* **34,** 741–756.e8 CrossRef Medline

41. Bragado Alonso, S., Reinert, J. K., Marichal, N., Massalini, S., Berninger, B., Kuner, T., and Calegari, F. (2019) An increase in neural stem cells and olfactory bulb adult neurogenesis improves discrimination of highly similar odorants. *EMBO J.* **38,** e98791 CrossRef Medline

42. Mohamed, T. M. A., Ang, Y. S., Radzinsky, E., Zhou, P., Huang, Y., Elfenbein, A., Foley, A., Magnitsky, S., and Srivastava, D. (2018) Regulation of cell cycle to stimulate adult cardiomyocyte proliferation and cardiac regeneration. *Cell* **173,** 104–116.e12 CrossRef Medline

43. Rando, T. A., and Blau, H. M. (1994) Primary mouse myoblast purification, characterization, and transplantation for cell-mediated gene therapy. *J. Cell Biol.* **125,** 1275–1287 CrossRef Medline

SASBMB